



## Real-Time Indoor Air Quality Index Prediction Using a Vacuum Cleaner Robot's AIoT Electronic Nose

Jutarut Chaoraingern<sup>1</sup>

Vittaya Tipsuwanporn<sup>2</sup>

Arjin Numsomran<sup>2\*</sup>

<sup>1</sup>Department of Robotics and AI Engineering, School of Engineering, King Mongkut's Institute of Technology Ladkrabang, Bangkok, Thailand

<sup>2</sup>Department of Instrumentation and Control Engineering, School of Engineering, King Mongkut's Institute of Technology Ladkrabang, Bangkok, Thailand

\* Corresponding author's Email: arjin.nu@kmitl.ac.th

---

**Abstract:** To encourage the good health and well-being sustainable development goal, this article presents the design and implementation of real-time indoor air quality index (AQI) prediction using an artificial internet of things (AIoT) electronic nose integrated into a vacuum cleaner robot. The objective of the proposed method is to implement an effective embedded AIoT solution utilizing sensor fusion and the TinyML framework for the purpose of strengthening the environmental health system with suitable current technology. The high-accuracy sensor outputs of total volatile organic compounds (TVOC), humidity, equivalent carbon dioxide (eCO<sub>2</sub>), and PM<sub>2.5</sub> gathered as the dataset are normalized in the data pre-processing state and utilized to create trained models using dense neural networks (DNN) deep learning algorithms. Tiny machine learning is responsible for neural network training, as it is capable of executing AI algorithms on embedded devices with extremely low power consumption and limited RAM and ROM resources. The testing results demonstrate that the predictive model performed well, with 99% accuracy for a maximum absolute regression error less than 15 and an 18.33 mean square error. The embedded device implementation uses Wio terminals with ARM Cortex-M4F microcontrollers for real-time indoor air quality index prediction and visualization. Experimental results demonstrating the average precision of the indoor AQI prediction were obtained at an average accuracy of over 98% with a computation time of 10 milliseconds and an acceptable usage of ROM and RAM resources of 8.5 KB and 1.1 KB, respectively, along with successive performances that satisfied web application data virtualization using the internet of things (IoT).

**Keywords:** AIoT, Deep learning, Embedded AI, Electronic nose, Indoor air quality index, TinyML.

---

### 1. Introduction

Air pollution is a major environmental health concern that can cause a variety of health problems. Air pollution is a combination of solid particles and gases that may be harmful to both humans and the environment. Long-term air pollution exposure can result in chronic respiratory disorders such as asthma and bronchitis [1, 2]. Children, the elderly, and persons with pre-existing illnesses are most sensitive to air pollution's health impacts [3, 4]. Furthermore, those who reside in places with high levels of air pollution are more likely to suffer from air pollution-related health issues [5, 6].

Electronic noses are a type of technology that detects and recognizes certain scents, chemicals, and entities in the environment [7]. The electronic noses equipped sensor arrays provide a comprehensive approach to capture the complex chemical composition of the air, enabling air pollution monitoring [8, 9].

To enhance the analytical capabilities of electronic noses by enabling compound separation and identification, gas chromatography have been integrated with air quality monitoring. In [10], the investigation of the responses of different electronic noses to odors emitted from a waste management plant was performed by combining results from



Figure. 1 AIoT electronic nose integrated in vacuum cleaner robot

dynamic olfactometry, gas chromatography, and mass spectrometry in order to implement a monitoring system and improve cleaner production technologies. For odorous air sample analysis, VOCs sensors with thermal desorption-gas chromatography-mass spectrometry (TD-GC-MS) were utilized for environmental measurement-based odor emissions [11].

Aside from the approaches stated above, regression analysis has been applied to electronic noses for determining air quality parameters. In electronic noses, the kernel SPXY data selection and support vector machines (SVM) regression techniques were used to produce a new approach to calibration transfer that delivered superior performance for air pollution measurement and monitoring systems [12]. The electronic nose system was presented as a method for recognizing the kind of sample gas and predicting its concentration using SVM and least squares regression [13].

To overcome the limitations of regression techniques, machine learning and deep learning have been developed to enhance the ability of the system to capture complex patterns and non-linear correlations in air quality data, resulting in improved air quality estimation accuracy [14]. With the goal of enhancing accuracy, ARIMA, Facebook Prophet, and LSTM machine learning models were suggested for predicting time series of PM<sub>2.5</sub> concentrations [15]. In [16], machine learning models including random forest, KNN, ridge and lasso, XGBoost, and AdaBoost were used to predict PM<sub>2.5</sub> pollutants in cities, thereby reducing error rates. Analyzing gas pollutant data with convolutional neural networks and improved long-short-term memory (CNN-ILSTM) was used to predict the AQI. The study demonstrated the effectiveness of deep learning in reducing training time dependencies and improving

AQI prediction accuracy [17]. Deep learning, which involves combining long-term and short-term memories in artificial neural networks, was demonstrated to be an effective method for forecasting air quality in the Madrid area [18]. The development of a cloud-based, real-time, in-vehicle air quality monitoring system was introduced in [19]. The article employed multilayer perceptron, support vector regression, and linear regression to accurately predict in-vehicle air quality indices by learning complex relationships between various factors affecting air quality. In addition, the investigation into the development of a real-time air quality monitoring system for utilizing within vehicles that makes use of machine learning prediction algorithms were discussed in [20]. This work provided insights for improving air quality prediction by using the machine learning algorithms long-short term memory (LSTM) and gated recurrent unit (GRU) for real-time prediction.

The previously stated research articles discuss the methodology of cloud-based machine learning or deep learning AQI prediction, which have internet-dependency limitations. Data transmission and processing in cloud-based systems rely on an internet connection. Problems with connectivity can disrupt real-time monitoring and predictions. The transmission of data to the cloud and its subsequent processing may impose latency. Monitoring in real time and immediate response may be affected.

To overcome the limitations of a cloud-based framework, this article proposes an embedded device-based artificial internet of things (AIoT) electronic nose that utilizes sensor fusion and the TinyML framework for real-time indoor air quality index prediction. The designed AIoT electronic nose integrated into a vacuum cleaner robot shown in Fig. 1 can process data locally, providing real-time AQI predictions without relying on internet connectivity while enabling immediate responses because local processing minimizes latency. The accuracy sensor outputs of total volatile organic compounds (TVOC), humidity, equivalent carbon dioxide (eCO<sub>2</sub>), and PM<sub>2.5</sub> are gathered as the dataset, normalized in the data pre-processing state, and used to create trained models for indoor air quality index prediction using deep learning algorithms based on dense neural networks (DNN).

The aim of this study is to implement an effective embedded AIoT solution utilizing sensor fusion and the TinyML framework for the purpose of strengthening the environmental health system with suitable current technology. The significance of article contributions is highlighted as follows:

- Indoor AQI real-time prediction using dense neural networks (DNN) deep learning algorithms:** the real-time indoor air quality index is predicted when the data from sensor fusion of TVOC, humidity, eCO<sub>2</sub>, and PM 2.5 are sensed by accurate sensors and carried through data pre-processing techniques, then processed by a DNN trained model. The result of indoor AQI prediction is demonstrated by the output of the neuron network, which ranges between 0-500 and conforms to the six bands of indoor AQI based on the EPA's Air Quality Index (AQI) and ISO 16000-29:2014 standard.
- Embedded AI deployment:** an AIoT electronic nose integrated into a vacuum cleaner robot using Wio terminals with an ARM Cortex-M4F embedded device that executed a neural network trained model for real-time indoor air quality index prediction and data visualization. TinyML TensorFlow Lite is used for neural network training, and the generated model is exported to an embedded device using an optimized compiler, allowing deep learning to execute on hardware with limited RAM and ROM resources.
- The internet of things (IoT):** IoT is integrated into an electrical nose module to create a network of connected systems on a cloud platform, allowing the module to communicate with a central data system and allow for more efficient demonstration and notification of indoor air quality index values via web applications.

The structure of this article is as follows: The second section describes the materials and methodology proposed. Experiments, results, analysis, and discussion are presented in the third section. Our conclusion is stated in the final section.

## 2. Materials and methods

### 2.1 AIoT electronic nose module

The AIoT electronic nose module in Fig. 2 is a combination of multi-sensor components listed in Table 1, including a total volatile organic compound (TVOC) sensor, an equivalent carbon dioxide (eCO<sub>2</sub>) sensor, a PM2.5 sensor, and a temperature-humidity sensor integrated into a Wio terminal embedded device with a powerful microcontroller, the ATSAMD51P19 with an ARM Cortex-M4F core running at 120 MHz, internet access via Realtek 2.4Ghz or 5Ghz Wi-Fi, a 2.4" LCD screen, and a Li-po battery chassis. The compact design of the

Table 1. List of AIoT electronic nose components

AIoT Electronic Nose Components	Total
SGP30 TVOC, eCO <sub>2</sub> sensor	1
HM3301 PM2.5 sensor	1
Temperature and humidity sensor	1
Wio terminal microcontroller	1
3.7 Volts Li-Po battery chassis	1



Figure. 2 AIoT electronic nose module

developed module is suitable for installation on a vacuum cleaner robot that moves around the specified area not only for cleaning purposes but also for checking and notifying the user of the air quality condition via IoT protocol and a warning message via a web application.

#### 2.1.1. Total volatile organic compound (TVOC) sensor

A total volatile organic compound (TVOC) sensor detects and quantifies the total concentration of VOCs in the air, including individual compounds as well as mixes of compounds used in a variety of applications.

Sensirion's SGP30 TVOC sensor module is suitable for indoor air quality applications because of its exceptional low power consumption and long-term stability. The total VOC concentration in the air is measured via the I2C interface to create a data set for a deep learning indoor AQI predictive model as well as real-time prediction. The sensor specifications are a 0 to 60000 ppb measuring range, 1 ppb resolution for the 0–2008 ppb measuring range, ±2 ppm accuracy, a long-term stability of ±2 ppm per year, and a low power consumption of 0.2 mA.

#### 2.1.2. Equivalent carbon-dioxide (eCO<sub>2</sub>) sensor

The quantity of equivalent carbon dioxide (eCO<sub>2</sub>) in the air is one of the most significant factors

Table 2. Sensor specifications

Sensor Type	Range	Accuracy
SGP30 TVOC	0 - 6000 ppb	15% of meas. value
SGP30 eCO <sub>2</sub>	0 - 1000 ppm	15% of meas. value
HM3301 PM <sub>2.5</sub>	1000 µg/ m <sup>3</sup>	1 µg/ m <sup>3</sup>
DHT11 Temperature	0 – 50 °C	±2%
DHT11 Humidity	20 – 90 %RH	±5 % RH

influencing the indoor air quality index. High levels of CO<sub>2</sub> can lead to poor air quality, which can cause health problems. Based on SGP30 multiple metal-oxide sensing technology, this module provides a fully calibrated eCO<sub>2</sub> output signal over the I2C interface. The output range is 400 ppm to 60000 ppm at a 1 HZ sampling rate. The minimum resolution is 1 ppm in the 400–1479 ppm measuring range.

### 2.1.3. PM<sub>2.5</sub> sensor

PM<sub>2.5</sub> is a term used to describe tiny particles in the air that are 2.5 micrometres or smaller in diameter. It can cause a range of health problems, including respiratory and cardiovascular diseases, as well as lung cancer. The indoor air quality index (AQI) is based on the concentration of PM<sub>2.5</sub> particles in the air. The higher the PM<sub>2.5</sub> concentration, the more polluted the air is. The technology for measuring PM<sub>2.5</sub> included in the HM3301 sensor is laser dust detection, which uses light scattering of the particle sensed by a photodiode to analyze the count concentration and mass concentration of the dust particles. Over the I2C interface, the HM3301 PM<sub>2.5</sub> sensor provides a maximum range of 1000 µg/ m<sup>3</sup> and 1 µg/ m<sup>3</sup> resolution.

### 2.1.4. Temperature and humidity sensor

A DHT11 temperature and humidity sensor has high accuracy, a wide measuring range, and long-term stability. It provides output through the built-in ADC in a humidity range of 5 to 95% RH with an accuracy of 5% and a temperature range of -20 to 60 °C with an accuracy of 2%. The measured values of temperature and humidity are not applied for indoor AQI predictive modelling but are used for absolute humidity compensation for the air quality signals (eCO<sub>2</sub> and TVOC) of the SGP30 sensor. Absolute humidity values (*d<sub>v</sub>*) in units of g/m<sup>3</sup> can be calculated by the following formula:

$$d_v(T, RH) = 216.7 \left[ \frac{\frac{RH}{100\%} \cdot 6.112 \cdot \exp\left(\frac{17.62 \cdot T}{243.12 + T}\right)}{273.15 + T} \right] \quad (1)$$

with T temperature and RH relative humidity.

The specifications of the SGP30 - Multi-gas (VOC and eCO<sub>2</sub>) sensor and PM<sub>2.5</sub> Sensor are listed in Table 2.

## 2.2 Real-time indoor air quality index (AQI) prediction

In Fig. 3, Indoor air quality index prediction models use data from TVOC, eCO<sub>2</sub>, and PM<sub>2.5</sub> sensors to generate a nonlinearly correlated set of air quality data. After normalization in the data pre-processing phase, the models utilize deep learning algorithms with dense neural networks (DNN) to predict the indoor air quality index. The prediction models are then compiled and downloaded to embedded devices in order to monitor the prediction results over short time frames. The real-time indoor air quality index prediction of the electronic nose module includes four major methodology compartments: dataset collection and pre-processing, a dense neural networks (DNN) predictive model, TinyML for embedded AI devices, and internet of things (IoT) integration.

### 2.2.1. Data collection, labelling and pre-processing

**1) Data collection:** In this study, the chamber size of 36x48.5x26.5 cm (25 liters) is used for environmental observation. The three designated gas parameters for sampling within the chamber are TVOC, eCO<sub>2</sub>, and PM<sub>2.5</sub>. One set of data acquisition will require seventeen minutes and will be repeated three times for each experiment. The experiment is carried out at a temperature of 32-33 °C and a humidity of 58-60%. Figs. 4-6 show the sampled data collection of TVOC, eCO<sub>2</sub>, and PM<sub>2.5</sub> concentrations inside the chamber, respectively. The sample gases, which vary in quantity of TVOC, eCO<sub>2</sub>, and PM<sub>2.5</sub>, influence the quality of the air within the chamber. The quantity of detected gas in the chamber was in the range of 0.8–1549.72 ppb for TVOC, 400–2807.96 ppm for eCO<sub>2</sub>, and 8.02–286.92 µg/ m<sup>3</sup> for PM<sub>2.5</sub>.

**2) Data labelling:** Assigning labels to sampled data points in order to train a model, the process of data labelling is explained by flowchart in Fig. 7. Reference to the USEPA’s Air Quality Index (AQI) [21] and ISO 16000-29:2014 standard [22], the indoor AQI is divided into six ranges, each of which has its own color code and explanation, as shown in Table 3. Indoor air quality index values are expressed as Eq. (2) [23-24].

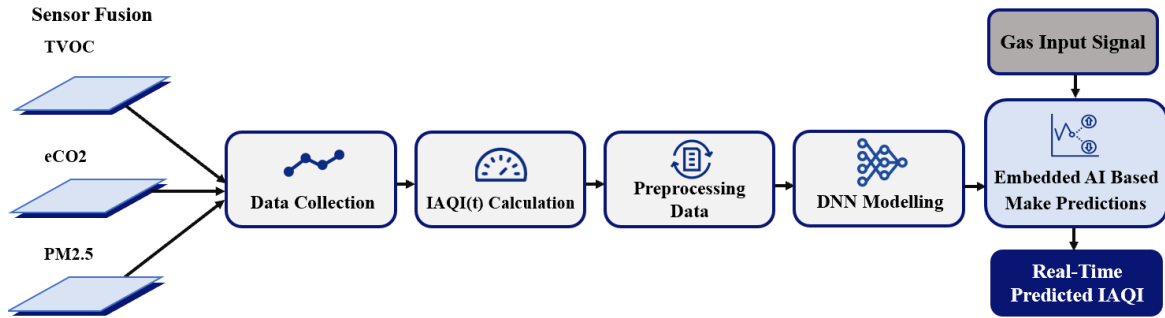


Figure. 3 Mechanisms of AIoT electronic nose indoor air quality index (AQI) prediction

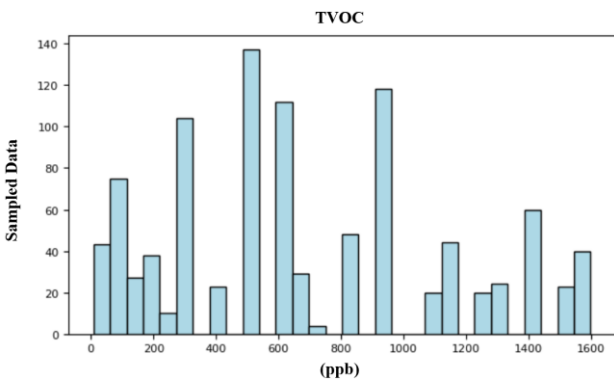


Figure. 4 TVOC sampled data collection

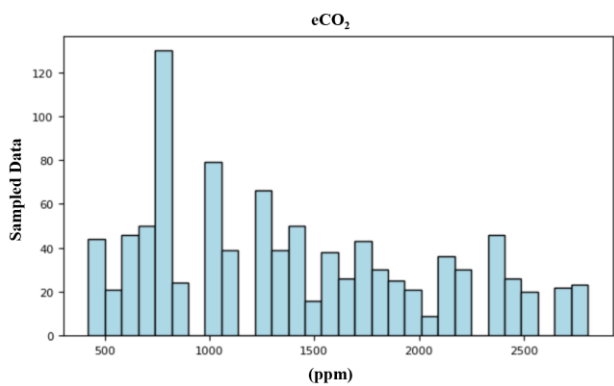


Figure. 5 eCO<sub>2</sub> sampled data collection

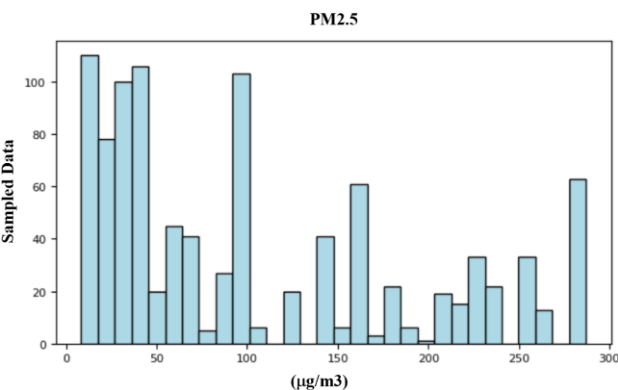


Figure. 6 PM 2.5 sampled data collection

$$I_p = \frac{I_{Hi} - I_{Lo}}{BP_{Hi} - BP_{Lo}} (C_p - BP_{Lo}) + I_{Lo} \quad (2)$$

$I_p$  is index for pollutant  $p$ .

$C_p$  is the rounded concentration of pollutant  $p$ .

$BP_{Hi}$  is the breakpoint greater than or equal to  $C_p$ .

$BP_{Lo}$  is the breakpoint less than or equal to  $C_p$ .

$I_{Hi}$  is the AQI value corresponding to  $BP_{Hi}$ .

$I_{Lo}$  is the AQI value corresponding to  $BP_{Lo}$ .

**3) Data pre-processing:** Data normalization technique, min-max scalar, has been applied in data pre-processing state to ensure that all data points have the same scale and range and make neural networks work better with the similar features' range. Eq. (3) shows the mathematical formula for the min-max scalar normalization method.

$$x_{scaled} = a + \frac{(x - \min(x))(b - a)}{\max(x) - \min(x)} \quad (3)$$

$x$  is the sampled data.

$[a, b]$  is rescale range.

### 2.3 Dense neural networks (DNN) Indoor AQI predictive modelling

This part explains the algorithms used to predict the future condition of the indoor air quality index when TVOC, eCO<sub>2</sub>, and PM2.5 signals are input to the electronic nose.

In Fig. 8 the functional sequence of dense neural network applied to the proposed a deep learning electronic nose is expressed. The designed neural network consists of 3 neurons on Input Layer (one per each input feature), 2 sequential hidden Dense Layers with 20 and 10 neurons with the Relu activation, and a one class output layer. There are 1000 epochs, and the learning rate is set to 0.0035. For validation during training, 20% of original train data will be put a part. The threshold of mean squared error (MSE) is not more than 15.

ReLU is the activation method used to enhance the output of the  $lth$  hidden layer as follows:

Table 3. Indoor AQI criteria

eCO <sub>2</sub> (ppm)	PM <sub>2.5</sub> (µg/m <sup>3</sup> )	TVOC (ppb)	Indoor AQI	6 Bands of Indoor AQI
C <sub>low</sub> -C <sub>high</sub>	C <sub>low</sub> -C <sub>high</sub>	C <sub>low</sub> -C <sub>high</sub>	I <sub>low</sub> -I <sub>high</sub>	
400-650	0-12	0-220	0-50	Good
651-1500	12.1-35.4	221-660	51-100	Moderate
1501-2000	35.5-55.4	661-1430	101-150	Unhealthy for sensitive group
2001-2500	55.5-150.4	1431-2200	151-200	Unhealthy
2501-5000	150.5-250.4	2201-3300	201--300	Very unhealthy
5001-15000	250.5-500	3301-5500	301-500	Hazardous

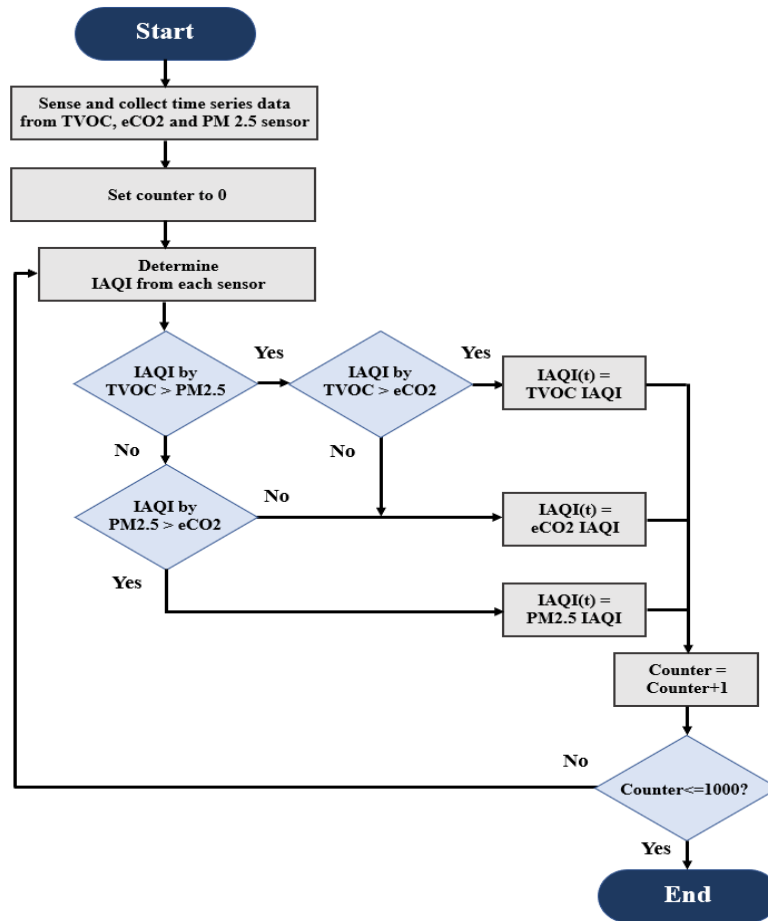


Figure. 7 Data labelling process

$$x_l = ReLU(W_l x_{l-1} + b_l) \tag{4}$$

$$ReLU(z) = \max(0, z) = \begin{cases} 0 & \text{for } z \leq 0 \\ z & \text{for } z > 0 \end{cases} \tag{5}$$

$x_0$  is input vector.  
 $x_l$  is output vector.  
 $W_l$  is weight matrix.  
 $b_l$  is bias vector.  
 $z$  is the vector of raw neural network outputs.

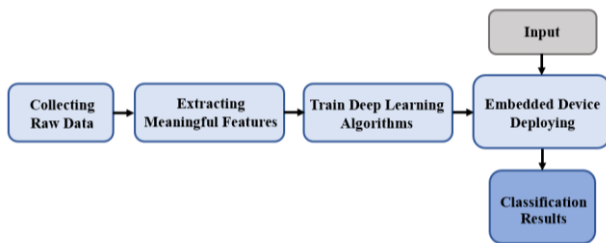
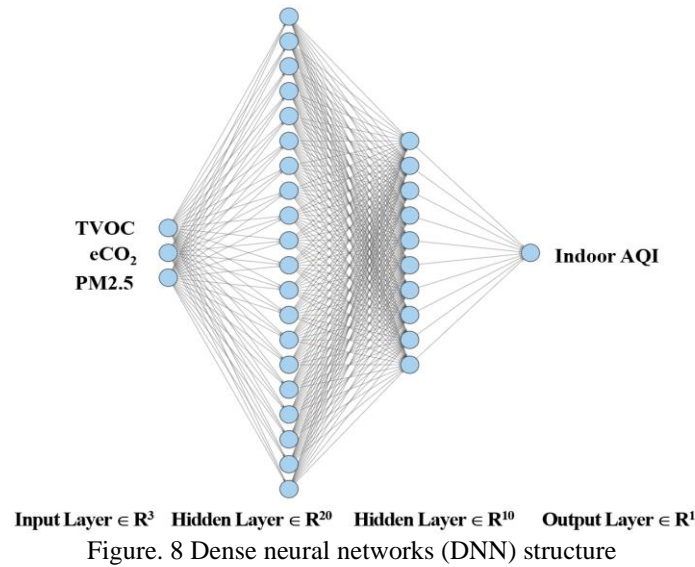
and coefficient of determination ( $R^2$ ) are used to assess the performance of the deep learning model employed to the electronic nose air quality prediction. Eqs. (6-9) present the formula for the evaluation metrics.

$$MSE = \frac{1}{n} \sum_{i=1}^n (y_i - \hat{y}_i)^2 \tag{6}$$

$$RMSE = \sqrt{\frac{1}{n} \sum_{i=1}^n (y_i - \hat{y}_i)^2} \tag{7}$$

$$MAE = \frac{1}{n} \sum_{i=1}^n |y_i - \hat{y}_i| \tag{8}$$

The mean squared error (MSE), root mean squared error (RMSE), mean absolute error (MAE),



$$R^2 = 1 - \frac{\sum_{i=1}^n (y_i - \hat{y}_i)^2}{\sum_{i=1}^n (y_i - \bar{y}_i)^2} \tag{9}$$

$\hat{y}_i$  is predicted value of  $y$ .  
 $\bar{y}_i$  is mean value of  $y$ .

### 2.4 TinyML for embedded AI device

TinyML is a machine learning approach that combines efficient and simplified machine learning applications [25]. It may be used to conduct artificial intelligence tasks in low-energy devices [26-27]. For AIoT electronic nose, the TinyML TensorFlow Lite framework on the Edge Impulse platform is used for training, optimizing, and deploying deep learning models to Wio terminal embedded device. The 4 keys steps workflow of TensorFlow Lite implementation for deep learning models can be expressed in Fig. 9.

These steps are:

- 1) Collecting raw data:** Connect with real time sensors for collecting the raw data.
- 2) Extracting meaningful features:** A method for reducing data dimensionality by identifying the most significant features from a dataset.
- 3) Train deep learning algorithms:** The process of building a model from a given dataset involves selecting the right algorithm, tuning the parameters of

the algorithm, and evaluating the performance of the model.

- 4) Deploying:** Build and deploy the program to embedded devices.

### 2.5 Internet of things (IoT)

The internet of things (IoT) is another function that is integrated to an electrical nose module for creating a network of connected system to cloud platform. IoT enables communication with central data system, allowing for more efficient monitoring and message notifying processes.

The Wio Terminal embedded device of AIoT electronic nose depicted in Fig. 10 is implemented for the IoT for data and prediction results visualization using MQTT (message queuing telemetry transport) protocol over Wifi to a Thingsboard cloud platform. The Wio Terminal is set up to connect to the MQTT broker running on the cloud platform. Once connected, it published the indoor AQI, TVOC, eCO<sub>2</sub>, PM2.5, temperature and humidity data being collected by the Thingsboard. The Wio Terminal's LCD display is then also used to show predicted indoor AQI, TVOC, eCO<sub>2</sub>, PM2.5, temperature and humidity data.

### 3. Experimental results and discussion

Regarding the designed dense neural network (DNN), there are 3 neurons on the input layer, 2 sequential hidden Dense Layers with 20 and 10 neurons with Relu activation, and an output layer with 1 class. The learning rate is set at 0.0035 and there are 1000 epochs total. Consequently, the trained model over training data has resulted in a loss of MSE in Fig. 11. Fig. 12 demonstrates the obtained 99%

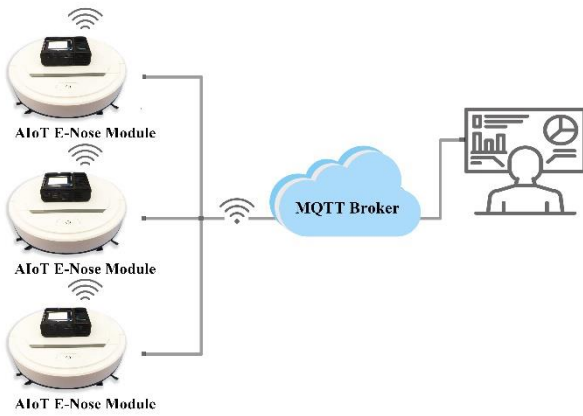


Figure. 10 Internet of things (IoT) feature

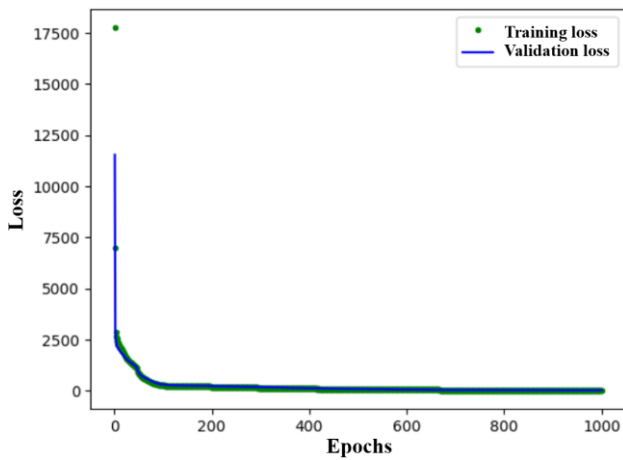


Figure. 11 Training and validation loss

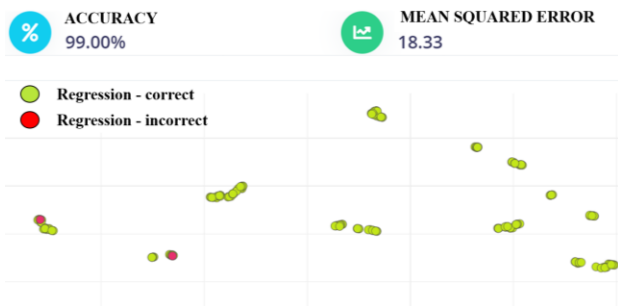


Figure. 12 Model testing results

Table 4. Comparison of prediction model results

	MSE	RMSE	MAE	R <sup>2</sup>
DNN	21.96	4.69	3.22	0.9947
SVM	26.69	5.17	1.83	0.9936
LR	1,254.75	35.42	28.29	0.6997

accuracy for a threshold setting of maximum absolute regression error less than 15 and a mean square error (MSE) of 18.33 when validating the model over validated data.

For model comparison, Google Colab was used to execute scripts. Using the various prediction models of dense neural networks (DNN), support vector machines (SVM) with a linear kernel type, and linear regression (LR) using Ordinary least squares (OLS), 100 data points were predicted.

Table 4 displays the validation results used to verify the prediction capability of the indoor AQI prediction models. Compared to other models, the DNN model had the highest R<sup>2</sup> and the lowest MSE, RMSE. The DNN prediction model had the most accurate predictions and superior generalization performance. The maximum R<sup>2</sup> obtained was 0.9947. The distributions of prediction results are depicted in Fig. 13 for simplicity of interpretation. The prediction model of the DNN exhibits similar shapes and tendencies to the actual indoor AQI data, as depicted by the graph. Additionally, the SVM prediction model displays a well-fitting line. The LR prediction model, however, does not match the actual data.

A DNN deep learning model was utilized to deploy to Wio Terminal, an ATSAM51-based microcontroller ARM Cortex-M4F CPU with a speed of 120 MHz, 192 KB of RAM, and 512 KB of ROM. Once the trained model was used to run on an embedded device, the experimental results of real-time indoor AQI prediction performance on the Wio Terminal, embedded device can be found in Fig. 14.

The validation results of the DNN trained models deployed to embedded device, Wio Terminal, are presented in Table 5 to ensure the accuracy of real-time embedded-based predictions. The average prediction performances are 95.55%, 99.22%, 99.08%, 98.11%, 97.99% and 98.49% respectively where the prediction for 6 indoor AQI bands are performed 10 times using different values of input validating features to get the average values.

According to the indoor AQI prediction results, the trained model AIoT electronic nose can satisfy the prediction performance with an average accuracy of over 98 % and an acceptable usage of resources of 8.5 KB in ROM and 1.1 KB in RAM. Important considerations for the real-time prediction model include high accuracy, low computation time, and minimal resource consumption. In addition, a comparison of the model's regression computation time for various prediction algorithms in edge computing is presented. The Edge Impulse platform demonstrated that the proposed indoor AQI required only 10 msec of regression computation time, whereas cloud-based AQI prediction in [19] required more computation time for both the SVM and LR prediction models.



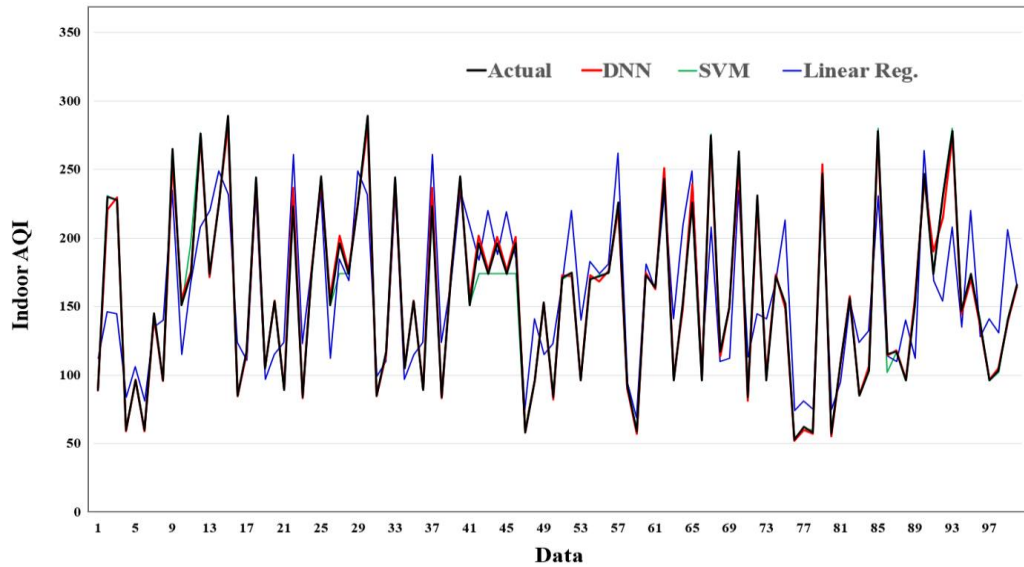


Figure. 13 The prediction of indoor AQI in DNN, SVM, and linear regression



(a)



(b)



(c)

Figure. 14 Real time indoor AQI predictive result: (a) Good, (b) Moderate, and (c) Less Unhealthy

Table 5. Average indoor AQI prediction performance

Indoor AQI Bands	Avg. Performance
Good	95.55%
Moderate	99.22%
Less Unhealthy	99.08%
Unhealthy	98.11%
Very Unhealthy	97.99%
Hazardous	98.49%

The result of the internet of things (IoT) is expressed in Fig. 15. The AIoT electronic nose uses a Wio terminal to connect to the MQTT broker running on the cloud platform. Once connected, it published the indoor AQI, TVOC, eCO<sub>2</sub>, PM2.5, temperature, and humidity data being demonstrated by the dashboard, while the high alarm threshold for the AQI index can be set for warning notifications on web applications.

#### 4. Conclusion

This article focused on investigating an essential approach for real-time indoor air quality index (AQI) prediction. By proposing an effective embedded AIoT solution utilizing sensor fusion and the TinyML framework of an electronic nose integrated into a vacuum cleaner robot, the sensor fusion outputs of total volatile organic compounds (TVOC), humidity, equivalent carbon dioxide (eCO<sub>2</sub>), and PM2.5 are normalized and utilized to create indoor AQI predictive models using deep learning algorithms employing dense neural networks (DNN). The neural network training is performed by tiny machine learning, which is capable of executing on-device data analytics with limited RAM and ROM resources

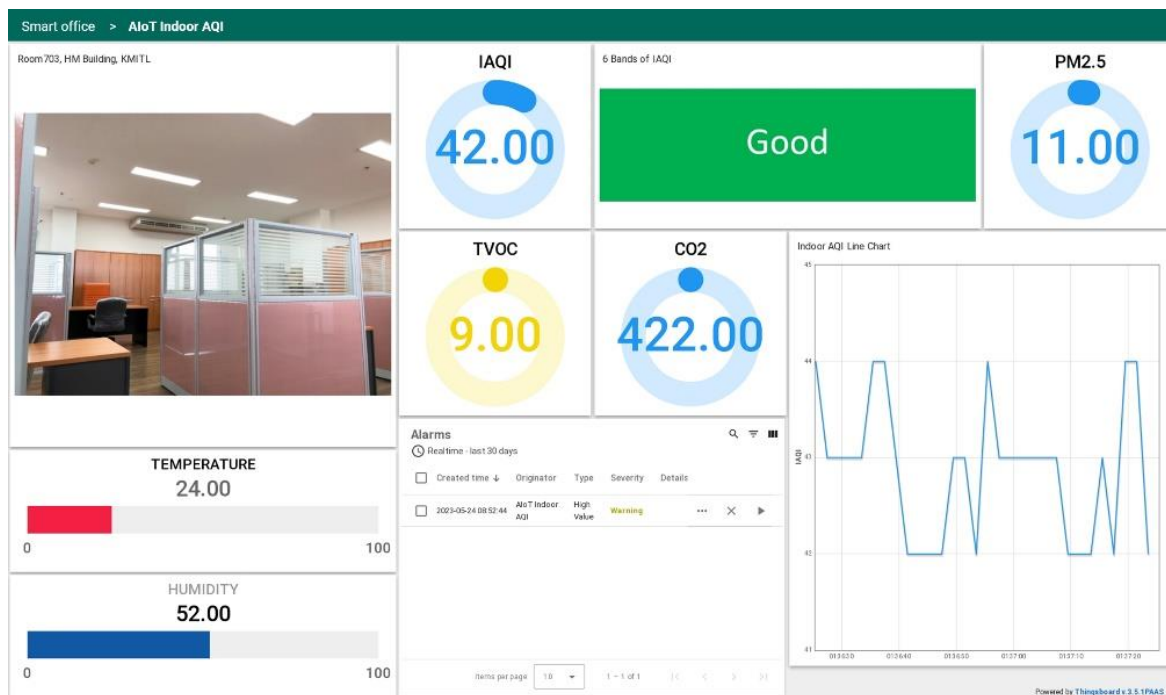


Figure. 15 IoT web application of real time indoor AQI AIoT electronic nose

on embedded devices. The embedded device implementation uses Wio terminals with ARM Cortex-M4F microcontrollers for real-time indoor air quality index prediction and visualization, extended with the further feature of the internet of things (IoT), which enables demonstrating and notifying the indoor air quality index values via web applications. Experiments indicated the achieved performance in prediction was reached with an average accuracy of over 98% at a regression computation time of 10 milliseconds and an acceptable usage of ROM and RAM resources of 8.5 KB and 1.1 KB, respectively. We hope that our research will be beneficial in solving the difficulty of on-device deep learning implementation as well as raising public awareness related to air pollution and environmental health. To further our research, we plan to augment the 3D mapping feature for creating a 3D map of its air pollution so that it applies to industrial applications.

**Conflicts of interest**

The authors declare no conflict of interest.

**Author contributions**

J. Chaoraingern and A. Numsomran established the research approach, did the calculations, and validated the proposed methodologies. V. Tipsuwanporn supervised J. Chaoraingern and A. Numsomran in their examination of a certain feature.

The findings were considered by all authors, who contributed to the final draft.

**References**

- [1] X. Li, L. Jin, and H. Kan, “Air Pollution: A Global Problem Needs Local Fixes”, *Nature*, Vol. 570, No. 7762, pp. 437-439, 2019.
- [2] E. K. Cairncross, J. John, and M. Zunckel, “A Novel Air Pollution Index Based on the Relative Risk of Daily Mortality Associated with Short-Term Exposure to Common Air Pollutants”, *Atmospheric Environment*, Vol. 41, No. 38, pp. 8442-8454, 2007.
- [3] M. Karthick, S. S. Kannan, and G. Velmathi, “Odour Sensor Based Solution for the Sanitary Problem Faced by Elderly People and Kindergarten Children”, *International Journal of Information Sciences and Techniques*, Vol. 4, No. 3, pp. 17-22, 2014.
- [4] C. Song, J. He, L. Wu, T. Jin, X. Chen, R. Li, P. Ren, L. Zhang, and H. Mao, “Health Burden Attributable to Ambient PM2.5 in China”, *Environmental Pollution*, Vol. 223, pp. 575-586, 2017.
- [5] S. Feng, D. Gao, F. Liao, F. Zhou, and X. Wang, “The Health Effects of Ambient PM2.5 and Potential Mechanisms”, *Ecotoxicology and Environmental Safety*, Vol. 128, pp. 67-74, 2016.
- [6] J. Choi, J. Y. Oh, Y. S. Lee, K. H. Min, G. Y. Hur, S. Y. Lee, K. H. Kang, and J. J. Shim,

- “Harmful Impact of Air Pollution on Severe Acute Exacerbation of Chronic Obstructive Pulmonary Disease: Particulate Matter is Hazardous”, *International Journal of Chronic Obstructive Pulmonary Disease*, Vol. 13, pp. 1053-1059, 2018.
- [7] L. Dentoni, L. Capelli, S. Sironi, R. Rosso, S. Zanetti, and M. Torre, “Development of an Electronic Nose for Environmental Odour Monitoring”, *Sensors*, Vol. 12, No. 11, pp. 14363-14381, 2012.
- [8] T. J. Alishba, M. Krishnan, R. N. David, and T. Antonio, “An Outlook of Recent Advances in Chemiresistive Sensor-Based Electronic Nose Systems for Food Quality and Environmental Monitoring”, *Sensors*, Vol. 21, No. 7, p. 2271, 2021.
- [9] T. Majchrzak, W. K. Wojnowski, T. Dymerski, J. Gębicki, and J. Namieśnik, “Electronic Noses for Indoor Air Quality Assessment”, *Electronic Nose Technologies and Advances in Machine Olfaction*, pp. 202-223, 2018.
- [10] P. Giungato, G. D. Gennaro, P. Barbieri, S. C. Briguglio, M. Amodio, L. D. Gennaro, and F. Lasigna, “Improving Recognition of Odors in a Waste Management Plant by Using Electronic Noses with Different Technologies, Gas Chromatography-Mass Spectrometry/Olfactometry and Dynamic Olfactometry”, *Journal of Cleaner Production*, Vol. 133, pp. 1395-1402, 2016.
- [11] M. Moufid, B. Bouchikhi, C. Tiebe, M. Bartholmai, and N. E. Bari, “Assessment of Outdoor Odor Emissions from Polluted Sites Using Simultaneous Thermal Desorption-Gas Chromatography-Mass Spectrometry (Td-Gc-Ms), Electronic Nose in Conjunction with Advanced Multivariate Statistical Approaches”, *Atmospheric Environment*, Vol. 256, p. 118449, 2021.
- [12] R. Laref, E. Losson, A. Sava, and M. Siadat, “Support Vector Machine Regression for Calibration Transfer between Electronic Noses Dedicated to Air Pollution Monitoring”, *Sensors*, Vol. 18, No. 11, p. 3716, 2018.
- [13] W. Khalaf, C. Pace, and M. Gaudio, “Least Square Regression Method for Estimating Gas Concentration in an Electronic Nose System”, *Sensors*, Vol. 9, No. 3, pp. 1678-1691, 2009.
- [14] G. K. Kang, J. Z. Gao, S. Chiao, S. Lu, and G. Xie, “Air Quality Prediction: Big Data and Machine Learning Approaches”, *International Journal of Environmental Science and Development*, Vol. 9, No. 1, pp. 8-16, 2018.
- [15] E. Gladkova and L. Saychenko, “Applying Machine Learning Techniques in Air Quality Prediction”, *Transportation Research Procedia*, Vol. 63, pp. 1999-2006, 2022.
- [16] D. Kothandaraman, N. Praveena, K. Varadarajkumar, B. M. Rao, D. Dhabliya, S. Satla, W. Abera, “Intelligent Forecasting of Air Quality and Pollution Prediction Using Machine Learning”, *Adsorption Science & Technology*, Vol. 2022, 2022.
- [17] J. Wang, X. Li, L. Jin, L. Jiazheng, Q. Sun, and H. Wang, “An Air Quality Index Prediction Model Based on CNN-ILSTM”, *Scientific Reports*, 2022.
- [18] R. Navares, and J. L. Aznarte, “Predicting Air Quality With Deep Learning LSTM: Towards Comprehensive Models”, *Ecological Informatics*, Vol. 55, 2020.
- [19] C. C. Goh, L. M. Kamarudin, A. Zakaria, H. Nishizaki, N. Ramli, X. Mao, S. M. M. S. Zakaria, E. Kanagaraj, A. S. A. Sukor, and M. F. Elham, “Real-Time In-Vehicle Air Quality Monitoring System Using Machine Learning Prediction Algorithm”, *Sensors*, Vol. 21, No. 15, p. 4956, 2021.
- [20] A. S. A. Sukor, G. C. Cheik, L. M. Kamarudin, X. Mao, H. Nishizaki, A. Zakaria, and S. M. M. S. Zakaria, “Predictive Analysis of In-Vehicle Air Quality Monitoring System Using Deep Learning Technique”, *Atmosphere*, Vol. 13, No. 10, p. 1587, 2022.
- [21] Guideline for Reporting of Daily Air Quality Air Quality Index (AQI): <https://nepis.epa.gov/Exe/ZyPDF.cgi/P100%206KOQ.PDF?Dockey=P1006KOQ.pdf/>
- [22] ISO 16000-29:2014, Indoor Air - Part 29: Test Methods for VOC Detectors: <https://www.iso.org/standard/55227.html/>
- [23] X. Tan, L. Han, X. Zhang, W. Zhou, W. Li, and Y. Qian, “A Review of Current Air Quality Indexes and Improvements Under the Multi-Contaminant Air Pollution Exposure”, *Journal of Environmental Management*, Vol. 279, p. 111681, 2021.
- [24] C. M. Payus, M. S. N. Syazni, and J. Sentian, “Extended Air Pollution Index (API) As Tool of Sustainable Indicator in the Air Quality Assessment: El-Nino Events with Climate Change Driven”, *Heliyon*, Vol. 8, No. 3, p. e09157, 2022.
- [25] G. Delnevo, S. Mirri, C. Prandi, and P. Manzoni, “An Evaluation Methodology to Determine the Actual Limitations of a Tinyml-Based Solution”, *Internet of Things*, Vol. 22, 2023.

- [26] P. P. Ray, “A Review on Tinyml: State-Of-The-Art and Prospects”, *Journal of King Saud University - Computer and Information Sciences*, Vol. 34, No. 4, pp. 1595-1623, 2022.
- [27] M. Rüb and A. Sikora, “A Practical View on Training Neural Networks in the Edge”, *IFAC-PapersOnLine*, Vol. 55, No. 4, pp. 272-279, 2022.